YSZ-$SrCo_{0.4}Fe_{0.6}O_{3-\delta}$ Membranes for the Partial Oxidation of Methane to Syngas

Xuehong Gu, Wanqin Jin, Changlin Chen, Nanping Xu, and Jun Shi
Membrane Science & Technology Research Center, Nanjing University of Technology, Nanjing 210009, P.R. China

Y. H. Ma
Center for Inorganic Membrane Studies, Dept. of Chemical Engineering, Worcester Polytechnic Institute, Worcester, MA 01609

The perovskite-related yttria-stabilized zirconia promoted $SrCo_{0.4}Fe_{0.6}O_{3-\delta}$ (SCFZ) oxides were used to construct membrane reactors for the partial oxidation of methane to syngas (POM). The oxygen permeability study of the SCFZ membrane in the air/helium gradient showed that the apparent activation energy was about 69 $\pm$ 5 kJ/mol at 1,023 $\sim$ 1,223 K, and the oxygen flux was controlled by the bulk diffusion and surface exchange rate. In a cofeed reactor packed with SCFZ pellets and a blank SCFZ membrane reactor without any catalyst packing, the SCFZ oxides showed low catalytic activity for POM in the fixed-bed reactor and no POM catalytic activity in the membrane reactor. An SCFZ membrane reactor with NiO/Al_2O_3 catalyst was continuously running for over 220 h under constant operational conditions. While about 64% of methane was converted with 100% CO selectivity after reaching the steady state, the oxygen flux was about 10 times the value of the air/helium gradient, in the reactor packed with the catalyst. The oxygen flux of SCFZ membranes in the reducing atmosphere could be limited by the surface reaction rate at the reaction side.

Introduction

In recent years, there has been a significant interest in a new approach to the partial oxidation of methane to syngas (POM), where a dense oxygen-permeable membrane is used to supply oxygen from air (Sanchez and Theodore, 1996; Dyer et al., 2000; Hendriksen et al., 2000; Gellings and Bouwmeester, 2000; Sammells et al., 2000). Several dense oxygen-permeable membranes, including dense stabilized zirconia membranes (Alqahtany et al., 1993), PbO dense films supported on a MgO-coated porous alumina tube (Omata et al., 1989), and perovskite-type or perovskite-related oxide membranes (Teraoka et al., 1985; Kruidhof et al., 1993; Pei et al., 1995; Qiu et al., 1995; Li et al., 1999a), have been investigated. Among these dense oxygen-permeable membranes, the perovskite-type or perovskite-related oxide membranes have been extensively investigated due primarily to their very high oxygen ionic and electronic conductivity at elevated temperatures and ability to separate oxygen from air without the use of an external electrical circuit.

There are a larger number of studies focusing on the preparation and performance investigation of perovskite-type oxide membranes. Teraoke et al. (1985) was the first to report the oxygen permeability through perovskite-type dense oxygen-permeable membranes. They concluded that the rate of oxygen permeation through $La_{1-x}Sr_xCo_{1-y}Fe_yO_{3-\delta}$ membranes increased with an increase in Sr or Co content. In particular, $SrCo_{0.8}Fe_{0.2}O_{3-\delta}$ oxides exhibited considerably high oxygen permeability, which was conformed by other investigators (Kruidhof et al., 1993; Qiu et al., 1995; Lee et al., 1997). However, since some of the high-oxygen-permeability perovskite-type oxides exhibited poor stability in a reduced-oxygen partial-pressure atmosphere at high temperatures (Kruidhof et al., 1993; Pei et al., 1995; Jin et al., 2000), they were not suitable for membrane reactor applications.

Correspondence concerning this article should be addressed to N. Xu. Current address of W. Jin: Institut für Physikalische Chemie, Universitä zu Köln, Luxemburger, str. 116, 50939 Köln, Germany.

Using $SrCo_{0.8}Fe_{0.2}O_{3-\delta}$ tubular membranes for POM, Pei et al. (1995) observed that the fracture of the tubular membrane occurred shortly after the initiation of the reaction. They concluded that the fracture happened because the lattice mismatch resulted from the phase change caused by the oxygen gradient across the membrane.

It is very important to select a suitable membrane material for constructing membrane reactors for the POM reaction. The ideal material for membrane reactors should have the following features: (1) high oxygen permeability; (2) good chemical stability under reducing atmosphere; and (3) a stable lattice structure under changes in O_2 partial pressure. Several reports have revealed that some perovskite-type or perovskite-related oxide membranes have exhibited chemical stability under POM reaction conditions. For example, Balachandran et al. (1997) reported nonperovskite oxides $SrFeCo_{0.5}O_x$ tubular membrane reactors packed with an Rh-based reforming catalyst for the POM. The $SrFeCo_{0.5}O_x$ membrane reactor was operated continuously for over 1,000 h, and an oxygen flux of 2–4 $cm^3/min \cdot cm^2$ was obtained during the reaction process. Tsai et al. (1997) also investigated disk-shaped perovskite-type $La_{0.2}Ba_{0.8}Fe_{0.8}Co_{0.2}O_{3-\delta}$ membrane reactors for the POM. They found that compared with the blank reactor, packing a 5% Ni/Al_2O_3 catalyst directly on the surface of the membrane reactor-side resulted in a fivefold increase in O_2 permeation and a fourfold increase in CH_4 conversion. Oxygen continuously transported from the air side appeared to have stabilized the membrane interior, and the $La_{0.2}Ba_{0.8}Fe_{0.8}Co_{0.2}O_{3-\delta}$ reactor was operated for up to 850 h. Recently, a novel perovskite-related oxide membrane, which was prepared by doping YSZ into $SrCo_{0.4}Fe_{0.6}O_{3-\delta}$ (SCFZ), has been reported in our laboratory (Li et al., 1999b; Li et al., 2001). The SCFZ membrane material exhibited very high oxygen permeability in air/helium gradient. High-temperature XRD in a flowing argon atmosphere showed that the SCFZ material was very stable in reduced oxygen partial pressures at high temperatures.

In this article, therefore, perovskite-related YSZ-promoted $SrCo_{0.4}Fe_{0.6}O_{3-\delta}$ membranes were used to study partial oxidation of methane to syngas. The partial oxidation reaction was performed over an extended period of time to investigate the chemical stability of the SCFZ membrane under reaction conditions. A detailed investigation was conducted to obtain the performance of the SCFZ membrane by carrying out the oxygen permeation measurements in the air/helium gradient and membrane reactions with and without the NiO/Al_2O_3 catalyst. In addition, SEM analysis was used to characterize the SCFZ membranes to demonstrate the structure changes of the used membranes.

Experimental Studies

Membrane preparation

The perovskite-related YSZ(9 wt %)$-SrCo_{0.4}Fe_{0.6}O_{3-\delta}$ (SCFZ) ceramic powders were synthesized by a solid-state reaction. Appropriate amounts of $SrCO_3$, Co_2O_3, Fe_2O_3 (the Second Chemical Industry of Shanghai, purity of 99.9%) and 8% Y_2O_3 stabilized ZrO_2 (YSZ) (Shenzhen Nanbo Structure Ceramics Co., Ltd.) were mixed and ball-milled in pure water for 24 h. After having been dried at 353 K for 24 h, the mixture was ground and calcined in air at 1,173 K for 10 h. The heating and cooling rates were controlled at 2 K/min. After the final calcination, the powders were ground and sifted to an average particle size of about 8 μm.

The disk-shaped SCFZ membranes were prepared by isostatic pressing at a pressure of 192 MPa using an oil press, which included loading, pressing, and ejecting. The green membrane disks were sintered in air at 1,513 K for 5 h in $MoSi_2$ furnace, with the heating and cooling rate controlled at 2 K/min. The sintered membranes were polished with a 1,000 MESH SiC before being used in experiments. The thicknesses of the membranes used in the oxygen permeation measurements were 0.44 mm, 1.16 mm, 1.80, mm and 2.32 mm. The disk-shaped membranes with the thickness of 1.80 mm were used for the membrane reactor study.

Catalyst preparation

The SCFZ particles employed in this study were prepared by pressing SCFZ powders with a particle size smaller than 50 μm at 256 MPa to form the pellets, which were then crushed and sieved to 20–40 mesh.

The 4.7 wt % NiO/Al_2O_3 catalyst was prepared by the impregnation techniques. An appropriate amount of γ-Al_2O_3 (20–40 mesh) was impregnated by an aqueous solution of $Ni(NO_3)_2 \cdot 6H_2O$ (the Second Chemical Industry of Shanghai; purity of 99.9%). After being dried at 333 K for 24 h, the catalytic precursors were calcined in air at 1023 K for 4 h. The color of the particles turned from green to dark blue after calcination. The BET surface area of the catalyst was 128 m^2/g.

Membrane reactor configurations and experimental procedures

Figure 1 shows the experiment apparatus used for oxygen permeation measurements and membrane reaction experiments. The detailed flow arrangements of three modes of operation, which included the oxygen permeation measurement, blank membrane reactor without any catalyst packing (briefly named blank membrane reactor), and membrane reactor with NiO/Al_2O_3 catalyst, are illustrated in Figure 2, which is similar to the one used by Tsai et al. (1997). A disk-shaped membrane between two gold rings was held in place

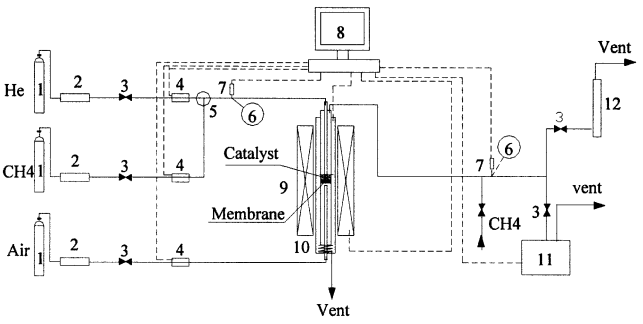

Figure 1. Membrane reaction apparatus.

1: gas cylinder, 2: gas dryer, 3: valve, 4: mass-flow controller, 5: mixer, 6: pressure gauge, 7: pressure sensor, 8: computer, 9: electric furnace, 10: membrane reactor, 11: chromatogram, 12: bubble flowmeter.

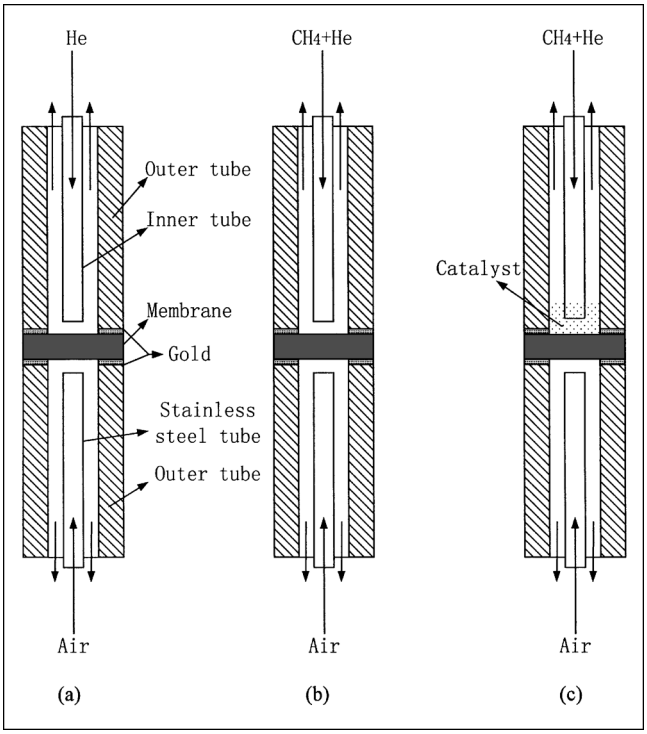

Figure 2. (a) Flow arrangement in oxygen permeation measurements; (b) blank membrane reaction experiments; (c) membrane reaction experiments.

by two quartz tubes (6 mm ID, 12 mm OD). The gold rings were the same dimensions as the quartz tubes, which left an effective area of about 0.283 cm^2 for the oxygen permeation. An inner quartz tube (2.3 mm ID, 4.3 mm OD) was used to introduce helium or a gas mixture of helium and methane to one side of the membrane, while a stainless-steel tube was used to introduce air to the other side of the membrane. In all cases of this study, air flow rates were controlled at 200 cm^3 (STP)/min. The clearance of the inner quartz tube and membrane surface was about 2–3 mm. Before the experiments were performed, the temperature around the SCFZ membranes was held at 1313 K for 10 h to ensure the softening of the gold rings. Gas leakage, if present, could be detected by monitoring the nitrogen concentration in the effluent from the oxygen-lean side of the membrane. The inlet gas flow rates were controlled by mass-flow controllers (Models D07-7A/ZM), which were calibrated by a bubble flowmeter. Both sides of the membrane were maintained at atmospheric pressure, which was monitored by electronic pressure sensors (Models DG1300). A programmable temperature controller (Model AI-708PA) controlled the temperature around the membrane, which was measured by a type-K thermocouple encased in an alumina thermocouple well. The effluent streams were analyzed by two on-line gas chromatographs (Model Shimadzu GC-7A and Model SP-6800) with about 1 cm^3 sample loop. The maximum sensitivity of the chromatographs was about 7000 mv·cm^3/mg (benzene). A 2-m 5A molecular sieve column was used for the separation of H_2, O_2, N_2, CH_4, and CO, and a 1-m TDX-01 column was used for the separation of CO_2 and hydrocarbons. The chromatograph with 5A molecular sieve was operated under a current of 180 mA and the attenuation of 1, under which a trace amount of oxygen (>1 Pa) could be detected. The analyses were checked by the carbon balance, which was within 5% for all reaction experiments. For oxygen permeation measurements, helium gas was used as the sweeping gas in the permeation side, and an internal standard gas CH_4 was added to the effluent streams and flowed through the on-line analysis loop. In the membrane reaction experiments, methane diluted by helium was introduced into the reaction side of the membrane, and the unreacted feed gases and products flowed through the loop of the on-line analysis. The conversion of CH_4 and selectivity of CO for the POM were defined, respectively, as follows

$$X_{CH_4} = \frac{F_{CH_4 inlet} - F_{CH_4 outlet}}{F_{CH_4 inlet}} \quad (1)$$

$$S_{CO} = \frac{F_{CO}}{F_{CH_4 inlet} - F_{CH_4 outlet}} \quad (2)$$

where F_i is the flow rate of species i, in mol/s. The oxygen flux in the dense membrane reactors could be calculated by the mass balance on the basis of the components of CO, H_2, CH_4, CO_2, O_2, and H_2O in exit stream

$$F_{O_2 inlet} = F_{O_2 outlet} + 1/2 F_{CO} + F_{CO_2} + F_{CH_4 inlet} - F_{CH_4 outlet} - 1/2 F_{H_2} \quad (3)$$

Characterization of membrane material

The crystal types of SCFZ powders were studied by XRD (Rigaku D/MAX-RB diffractometer, with CuKα radiation). The sintered and used membranes were characterized by SEM (JSM-6300). The relative densities of the sintered membranes were determined by the Archimedes method, and exceeded 90% of the theoretical density in all cases.

Results and Discussion

Oxygen permeability

The oxygen permeation fluxes through the SCFZ membrane disks with the thickness of 0.44 mm, 1.16 mm, and 2.32 mm were measured as a function of temperature in air/helium gradient. The flow rate of the sweep gas, He, was controlled at 50 cm^3(STP)/min first. After helium was initially introduced, the oxygen flux decreased with time, and required about 2 h to attain the steady state. This phenomenon was most likely caused by the release of the lattice oxygen from the membrane bulk when the helium was first introduced, and the rate of the release of the lattice oxygen decreased gradually and finally reached the steady value when the steady oxygen vacancy was fully developed in the bulk of the membrane. A similar phenomenon was reported by Tsai et al. (1997) and Zeng et al. (1998). The steady oxygen permeation data were used to calculate the activation energy. The Arrhenius plots of three thicknesses are shown in Figure 3. The oxygen partial pressure difference across the membrane was

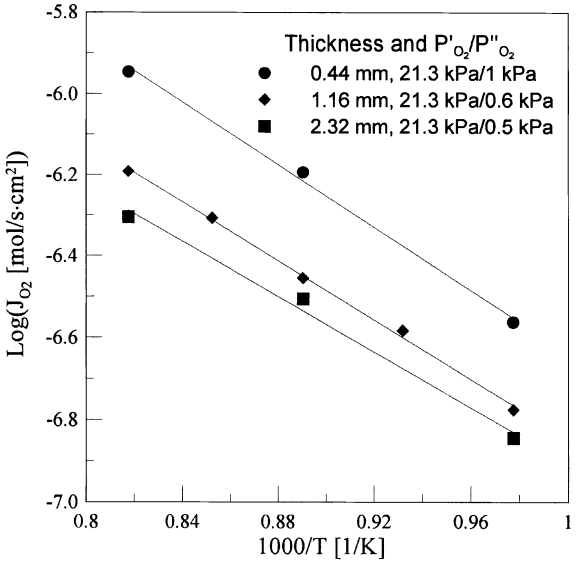

Figure 3. Temperature dependence of oxygen permeation flux in air/helium gradient for different membrane thicknesses.

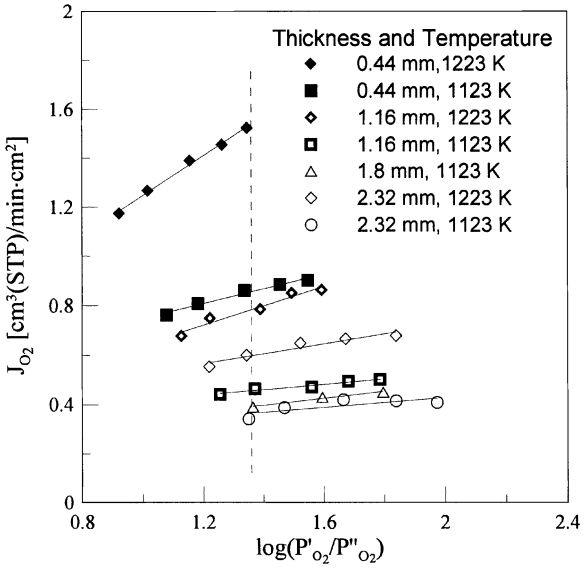

Figure 4. Oxygen pressure dependence of the oxygen permeation flux air/helium gradient for different membrane thicknesses at 1,123 and 1,223 K.

fixed during measurement. These straight lines in Figure 3 have approximately the same slope, giving the apparent activation energy of 69 ± 5 kJ/mol between 1023 and 1223 K, which was similar to that of the SCFZ prepared with nitrate precursors by Li et al. (1999b).

Four SCFZ membranes with a thickness of 0.44 mm, 1.16 mm, 1.8 mm, and 2.32 mm were used to investigate the thickness dependence of the oxygen flux. The experimental results at 1,123 K and 1,223 K are shown in Figure 4. The data points near to the vertical line in Figure 4 were used to investigate the thickness dependence of the oxygen flux, which is showed in Figure 5a. As expected, it can be seen from Figure 5a that the oxygen flux increased as the thickness of the membrane was decreased. When the oxygen permeation is controlled by the bulk diffusion, the oxygen flux can generally be described by the Wagner's equation (1975)

$$J_{O_2} = -\frac{RT}{4^2F^2L}\int_{\ln P'_{O_2}}^{\ln P''_{O_2}} t_{el}\sigma_{\text{ion}}\, d\ln P_{O_2} \qquad (4)$$

where R is the gas constant; L is the thickness of membrane; F is the Faraday constant; P'_{O_2} and P''_{O_2} are the oxygen partial pressures at the high and low pressure side of the membrane, respectively; t_{el} is the electronic transference number; and σ_{ion} is the ion conductivity. Therefore, according to Eq. 4, the oxygen permeation flux should be inversely proportional to the membrane thickness if the transport of the oxygen ion is limited by the bulk diffusion. However, departures from this ideal inverse relationship were observed in Figure 5a. To further substantiate this deviation from the ideal inverse relationship, a log-log plot of J_{O_2} vs. 1/L is shown in Figure 5b. Both lines have the same slope of around 0.57, an indication that the permeation flux is at least partially controlled by the surface exchange rate (Chen et al., 1997).

Catalytic performance of SCFZ membrane material

In order to study the SCFZ membrane reactors packed with NiO/Al_2O_3 catalyst, the SCFZ blank membrane reactor without any catalyst packing was investigated first. The blank membrane reactor was operated at 1,123 K, with a CH_4 flow rate of 2.9 cm^3(STP)/min and a helium flow rate of 17.9 cm^3(STP)/min. The reaction was run continuously for over 270 h. The main reaction products were CO_2 and H_2O, and no C_2, CO, and H_2 were detected. The results of the blank membrane reaction experiments are shown in Figure 6. For comparison, before methane was introduced, the steady-state oxygen flux under the air/helium gradient (air on one side and helium used as the sweep) was determined to be 0.4 cm^3(STP)/min $\cdot$ cm^2, at the helium flow rate of 17.9 cm^3(STP)/min and 1,123 K. However, once the methane and helium mixture was introduced to one side of the membrane, the oxygen flux increased with the increase of methane conversion and the oxygen partial pressure in the reaction side decreased gradually. When the reaction time was close to 270 h, a steady-state oxygen flux of about 0.8 cm^3(STP)/min $\cdot$ cm^2 was reached. At this time, the oxygen partial pressure in the reaction side was around 15 Pa.

Tsai et al. (1997) performed a similar experimental study of disk-shaped $La_{0.2}Ba_{0.8}Fe_{0.8}Co_{0.2}O_{3-\delta}$ membrane without catalyst packing, and obtained about 5% CH_4 conversion. Their reaction products, consisting of CO_2, CO, and C_2, were different from our experimental results due, possibly, to the difference between the catalytic activities of SCFZ membrane and their $La_{0.2}Ba_{0.8}Fe_{0.8}Co_{0.2}O_{3-\delta}$ membrane.

A fixed-bed reactor packed with 0.3-g SCFZ particles was used to further investigate the catalytic activity of SCFZ. A mixture of 4.9 cm^3(STP)/min methane, 31.6 cm^3(STP)/min helium, and 6.5 cm^3(STP)/min air (oxygen partial pressure of 3.2 kPa) was introduced into the reactor. The reaction tem-

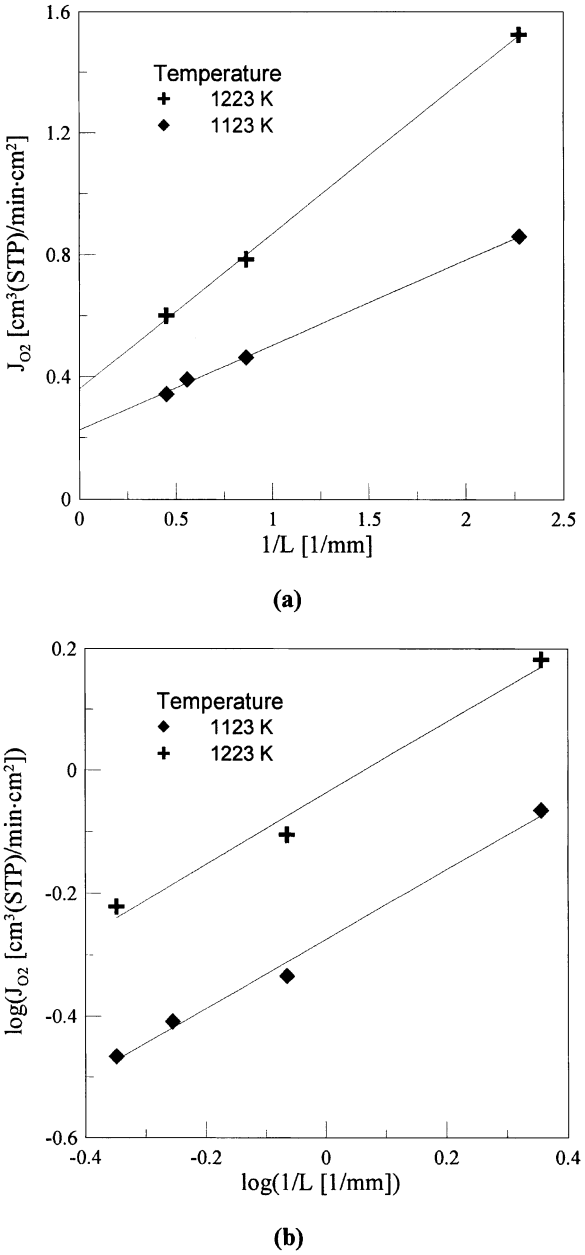

Figure 5. Thickness dependence of the oxygen permeation flux at the same oxygen partial pressure gradient at 1,123 and 1,223 K.

(a) J_{O_2} vs. 1/L; (b) log J_{O_2} vs. log (1/L).

perature was kept at 1133 K and the effluent gases at the outlet of the reactor included H_2, CO, CO_2, O_2, and H_2O, but no C_2 was detected. The results suggested that the SCFZ material exhibited some catalytic activity for POM, but poor catalytic activity for oxidative coupling of methane (OCM). The results of the fixed-bed reaction packed with SCFZ particles are shown in Figure 7. A gradual increase in methane conversion, as well as CO selectivity, was observed at the initial stage (first 20 h), which was due to an increase in the catalytic activity of the SCFZ particles during this period. When a steady state was reached, the CH_4 conversion of 30%,

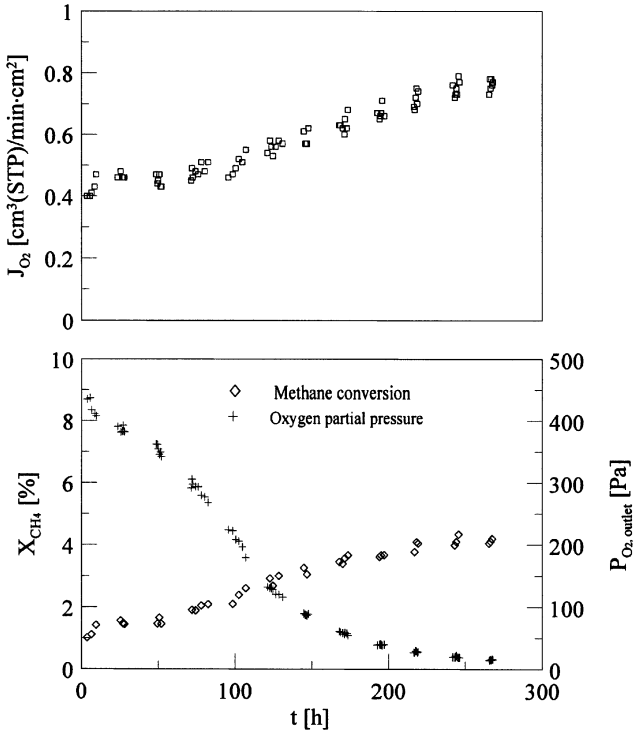

Figure 6. Long-time stability of the blank membrane reactor at 1,123 K.

Membrane thickness: 1.8 cm. Feeding conditions: Q_{CH_4} = 2.9 cm³ (STP)/min, Q_{He} = 17.9 cm³ (STP)/min.

CO selectivity of 70%, and H_2/CO ratio of about 2.2 were obtained. Chromatograph analysis showed that the partial pressure of the unreacted oxygen in the effluent gas was about 150 Pa.

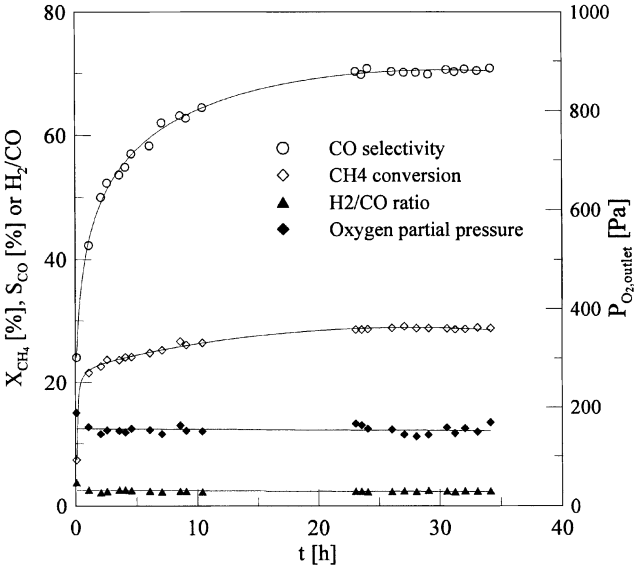

Figure 7. Stability of the fixed-bed reactor packed with SCFZ particles at 1,133 K.

Feeding conditions: Q_{CH_4} = 4.9 cm³ (STP)/min, Q_{He} = 31.6 cm³ (STP)/min, Q_{air} = 6.5 cm³ (STP)/min.

Like the fixed-bed reactor, the catalytic activity of the membrane surface, which was exposed to the methane side, gradually increased during the 270-h operation. As shown in Figure 6, the increase in catalytic activity at the membrane surface could enhance the interaction of oxygen ion with gas species and contribute to an increase in oxygen flux. A detailed discussion is given in the section "Comparison and Analysis of Oxygen Permeation in Three Processes."

Membrane reaction with NiO/Al_2O_3 catalyst

Long-term experiments performed in a fixed-bed reactor packed with 0.1 g 4.7 wt % NiO/Al_2O_3 catalyst showed steady catalytic activity with a CH_4 conversion, CO selectivity, and H_2/CO of about 86.7%, 100%, and 1.75 respectively, at the feed flow rates of 2.9 cm^3(STP)/min CH_4, 6.2 cm^3(STP)/min air, and 17.9 cm^3(STP)/min He. Since experimental results from the fixed-bed reactor studies showed that the catalytic activity of the SCFZ particles was relatively low compared to that of the NiO/Al_2O_3 catalyst, the SCFZ particles were not selected for the membrane reactor experiments.

A fresh SCFZ disk-shaped membrane reactor packed with 0.1 g 4.7 wt % NiO/Al_2O_3 catalyst was used to investigate the POM at 1,123 K. The membrane reactor was continuously operated for over 220 h at constant feed flow rates of 2.9 cm^3 (STP)/min CH_4, 17.9 cm^3 (STP)/min helium, and 200 cm^3 (STP)/min air. The effluent stream contained the products of CO, CO_2, H_2, H_2O, and unreacted CH_4 and O_2. The reaction results for 220 h are shown in Figure 8. At the initial stage, the CH_4 conversion and CO selectivity decreased within a short period of time; then, the CH_4 conversion and CO selectivity increased gradually to about 64% and 100% at 60 h, and the oxygen flux was about 4.5 cm^3 (STP)/min·cm^2, which was about 10 times the value in air/helium gradient at the same temperature. The variations in methane conversion and CO selectivity in the first 60 h could be attributed to a reduction in NiO/Al_2O_3 and an increase in oxygen flux, as shown in Figure 8. A similar increase in the oxygen flux was reported by Tsai et al. (1997), although their reactor was operated under oxygen-limited conditions and the oxygen permeation flux was controlled by the bulk diffusion for their membrane. When the reaction time was greater than 60 h, slight decreases in the oxygen flux and CH_4 conversion were found, due, possibly, to the final readjusting of the lattice structure. Steady state in the membrane reactor was reached after about 150 h.

Comparison and analysis of oxygen permeation in three processes

In order to further study the oxygen permeability of the SCFZ membrane in the reactive atmosphere, three processes were compared at 1123 K. These included the oxygen permeation measurement, blank membrane reaction experiment, and membrane reaction experiment with NiO/Al_2O_3 catalyst. The thickness of the membranes adopted in the experiments was 1.8 mm. All the data of the oxygen flux used for a comparison were measured after steady state was reached. For the membrane reactors, the methane flow rates were controlled at a constant rate of 2.9 cm^3 (STP)/min, and the oxygen fluxes were measured at different helium flow rates. The value of oxygen partial pressure at the lean-oxygen side was obtained by chromatographic analysis. For every operating condition, the measurement was repeated more than three times, and the average values were used for experimental comparison. For the oxygen permeation measurement in air/helium gradient and the blank membrane reaction, the error bars of P''_{O_2} values were lower than 5%, and for the membrane reaction, the error bars of P''_{O_2} values were lower than 10%. The results of the three experiments are shown in Table 1.

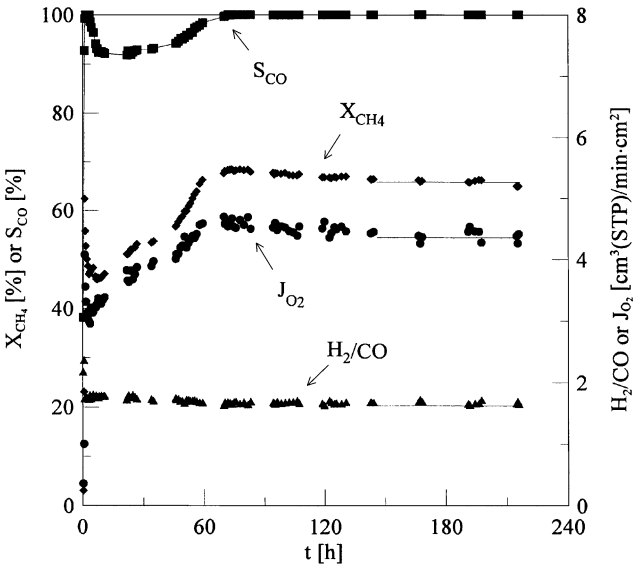

Figure 8. Long-time stability of the membrane reactor packed with NiO/Al_2O_3 catalyst at 1,123 K.

Membrane thickness: 1.8 cm. Feeding conditions: Q_{CH_4} = 2.9 cm^3 (STP)/min, Q_{He} = 17.9 cm^3 (STP)/min.

For the oxygen permeation measurement in the air/helium gradient, the oxygen partial pressure at the permeation side dropped along with an increase in the oxygen flux when the helium flow rate was increased, as shown in Table 1. This was because the decrease in the oxygen partial pressure at the permeation side brought about an increase in the gradient of the oxygen chemical potential across the membrane, which resulted in an increase in the oxygen flux. From Table

Table 1. Comparison of Oxygen Fluxes at 1,123 K among Three Experimental Processes

	Oxygen Permeation Exp.		Blank Memb. Reaction		Memb. Reaction	
Q_{He}, cm^3 (STP)/min	J_{O_2}, cm^3 (STP)/min·cm^2	P''_{O_2}, Pa	J_{O_2}, cm^3 (STP)/min·cm^2	P''_{O_2}, Pa	J_{O_2}, cm^3 (STP)/min·cm^2	P''_{O_2}, Pa
17.9	0.39	9.2×10^2	0.77	1.5×10^1	4.35	6.9
32.2	0.43	5.4×10^2	0.69	2.9×10^1	3.87	4.8
50.4	0.45	3.4×10^2	0.60	6.1×10^1	3.44	1.9

1, however, it is interesting to note that the oxygen flux in both the blank membrane reactor and the membrane reactor decreased with an increase in helium flow rate. However, the dependences of the oxygen partial pressure on the helium flow rate in the permeate side were different between the two types of membrane reactors. For the blank membrane reactor, the oxygen partial pressure at the reactive (permeate) side increased with an increase in the helium flow rate; while for the membrane reactor, the oxygen partial pressure decreased when the helium flow rate increased.

Previous reports (van Hassel et al., 1994; Xu and Thomson, 1997) in the literature have shown that the oxygen flux of some membrane materials is limited by the rate of the surface reaction in a reducing atmosphere. Ten Elshof et al. (1995) found that for $La_{1-x}Sr_xFeO_{3-\delta}$ ($x = 0.1$–0.4) membranes, the oxygen permeation flux was controlled mainly by the bulk-diffusion in air/helium gradients. However, when $La_{1-y}Sr_yFeO_{3-\delta}$ ($y = 0.1$, 0.2) membranes were in large oxygen partial-pressure gradients (air/CO, CO_2 mixture), the oxygen flux was limited by the carbon monoxide oxidation rate at a low oxygen partial pressure (van Hassel et al., 1994). Xu and Thomson (1997) found that the oxygen flux in their disk-shaped $La_{0.6}Sr_{0.4}Co_{0.2}Fe_{0.8}O_{3-\delta}$ catalytic membrane reactors for the oxidative coupling of methane were significantly higher than that in air/N_2 gradient. They postulated that it was possible that the oxygen fluxes were limited by the surface exchange rates at the oxygen-lean side of the membrane for OCM.

It has been mentioned in the section on "Catalytic Performance of SCFZ Membrane Material" that the POM reaction occurred in the fixed-bed reactor packed with SCFZ particles, while only methane combustion took place in the blank-membrane experiments. This implied that the catalytic performance of the oxygen species released from the SCFZ membrane was somewhat different from that of oxygen adsorbed from the gas phase. In other words, the oxygen adsorbed on the SCFZ surface mainly contributed to the POM reaction in the fixed-bed reactor, whereas the lattice oxygen on the membrane surface contributed to the methane combustion in the blank-membrane experiments. Similarly, for the membrane reaction experiments with NiO/Al_2O_3, the methane combustion reaction should occur between methane and the lattice oxygen ion; meanwhile at the membrane surface, there were reactions between lattice oxygen ions and the reducing gases of CO and H_2 from reforming reactions in the NiO/Al_2O_3 catalyst bed. It can therefore be postulated that the surface oxygen ions exposed to the reducing atmosphere could be transformed by four routes described below by adopting the Kröger–Vink notation (Kröger, 1964)

$$CH_4 + 4O_O^X + 8h^{\cdot} \rightarrow CO_2 + 2H_2O + 4V_O^{\cdot\cdot} \quad (5)$$

$$CO + O_O^X + 2h^{\cdot} \rightarrow CO_2 + V_O^{\cdot\cdot} \quad (6)$$

$$H_2 + O_O^X + 2h^{\cdot} \rightarrow H_2O + V_O^{\cdot\cdot} \quad (7)$$

$$2O_O^X + 4h^{\cdot} \rightarrow O_2 + 2V_O^{\cdot\cdot} \quad (8)$$

In the blank-membrane reactor, Eqs. 5 and 8 occurred at the membrane surface, and the oxygen flux was enhanced by Eq. 5 compared with the oxygen permeation measurement. When the flow rate of methane was controlled at a constant rate, the increase in the helium flow rate would result in a decrease in the methane partial pressure in the reactive side. Therefore, from the viewpoint of the reaction kinetics, the rate of the reaction in Eq. 5 would decrease, which would eventually lead to the decrease in the oxygen flux. For the membrane reactor with NiO/Al_2O_3 catalyst packing, there were larger amounts of reducing gases such as CO, H_2, and CH_4 in the reaction side. Reactions in Eqs. 5–8 would occur simultaneously at the membrane surface. Because of the stronger reducing potential of H_2 and CO, the rates of the reactions in Eqs. 6 and 7 were essentially higher than that of the reaction in Eq. 5. Consequently, the oxygen flux of the membrane reactor packed with the catalyst would be substantially higher than that of the membrane reactor without the catalyst. A decrease in the oxygen flux with an increase in the helium flow rate in the membrane reactor with NiO/Al_2O_3 catalyst could be attributed to the decrease in the rates of reaction in Eqs. 5–7, which was similar to the result of the blank-membrane reactor without the catalyst.

In the blank-membrane reactor and the membrane reactor with catalyst, there were two competing phenomena when the helium flow rate was increased: (a) increasing flow rates tended to maintain lower oxygen pressures at the reactive side; (b) increasing flow rates also lowered the methane partial pressure, which would lower the rate of reaction in Eq. 5 for the blank-membrane reactor or the rates of surface reactions and POM reaction for the membrane reactor with catalyst, thus, improving the amount of molecular oxygen in the reactive side of the membrane. These two competing processes could raise or lower the oxygen pressure, depending on their relative effects. As shown in Table 1, the increase in oxygen partial pressure with the increase of the helium flow rate in the blank-membrane reactor might mainly be attributed to the decrease in the reaction rates in the reactor [process (b)]; while in the membrane reactor with catalyst, the decrease in the oxygen partial pressure might mainly be attributed to the dilution of helium [process (a)].

For a further examination of the effect of the surface-exchange on the oxygen flux in the membrane reactor with catalyst packing, the effect of the methane partial pressure on the oxygen flux was investigated at five different feed conditions. The results are shown in Figure 9. It was seen that the increase in the methane partial pressure in the inlet of the reactor caused an increase in the oxygen flux. The results again suggested that the oxygen flux of the SCFZ membrane in the reducing atmosphere should be limited by the rate of the surface exchange.

XRD and SEM analyses of SCFZ membranes

The XRD pattern of the SCFZ membrane material is illustrated in Figure 10. For comparison, an XRD pattern of $SrCo_{0.4}Fe_{0.6}O_{3-\delta}$ oxides prepared by solid-state reaction is also shown in this figure. As can be seen, the $SrCo_{0.4}Fe_{0.6}O_{3-\delta}$ oxides have a pure cubic perovskite phase structure, and the SCFZ is a multiphase material composed of $SrZrO_3$, ZrO_2, and perovskite phase similar to $SrCo_{0.4}Fe_{0.6}O_{3-\delta}$ oxides. However, the Bragg angles of the perovskite phase in the SCFZ are slightly lower than those of the $SrCo_{0.4}Fe_{0.6}O_{3-\delta}$ oxides, indicating that most Y^{3+} and

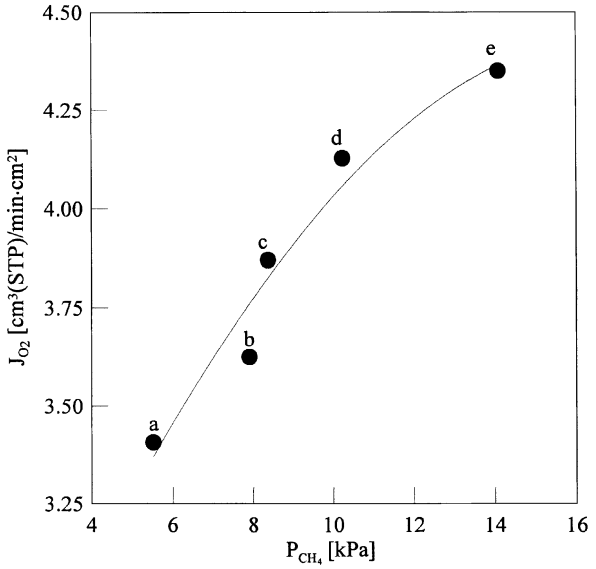

Figure 9. Effect of methane partial pressure on oxygen flux in SCFZ membrane reactor packed with NiO/Al_2O_3 at 1,123 K.

Feeding conditions: (a) $Q_{CH_4} = 2.9$ cm^3 (STP)/min, $Q_{He} = 50.4$ cm^3 (STP)/min; (b) $Q_{CH_4} = 1.5$ cm^3 (STP)/min, $Q_{He} = 17.9$ cm^3 (STP)/min; (c) $Q_{CH_4} = 2.9$ cm^3 (STP)/min, $Q_{He} = 32.2$ cm^3 (STP)/min; (d) $Q_{CH_4} = 2.0$ cm^3 (STP)/min, $Q_{He} = 17.9$ cm^3 (STP)/min; (e) $Q_{CH_4} = 2.9$ cm^3 (STP)/min, $Q_{He} = 17.9$ cm^3 (STP)/min.

some Zr^{4+} in the SCFZ could have entered the lattice positions of the perovskite phase (as Y^{3+} and Zr^{4+} have a larger ionic radius than Co^{3+} and Fe^{3+}, which contributed to the increase in the crystal cell volume of the perovskite phase). A detailed XRD investigation on the SCFZ material can be found in Li et al. (2001). Figure 11 shows the SEM photos of the fresh and used membranes. It is seen from Figure 11a that significant grain boundaries existed in the bulk of the fresh membrane. After being polished by 1000 MESH SIC, a smooth membrane surface (shown in Figure 11b) was obtained. For the blank membrane reactor, a slight deterioration in the structure of the membrane surface exposed to the reaction side (Figure 11c) occurred. However, for the used

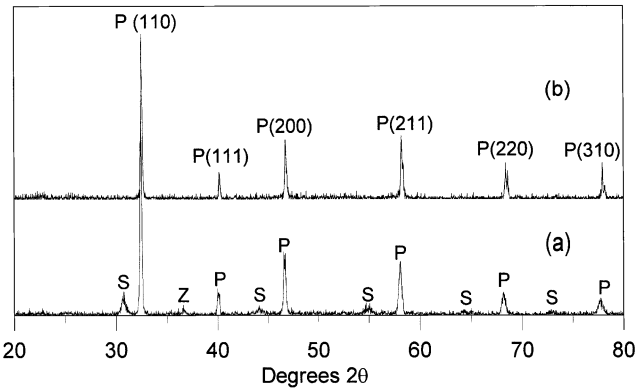

Figure 10. (a) X-ray diffraction patterns of SCFZ membrane material; (b) $SrCo_{0.4}Fe_{0.6}O_3$ oxides.

P (hlk): Perovksite (Mill's indexes); (Z) ZrO_2; (S) $SrZrO_3$.

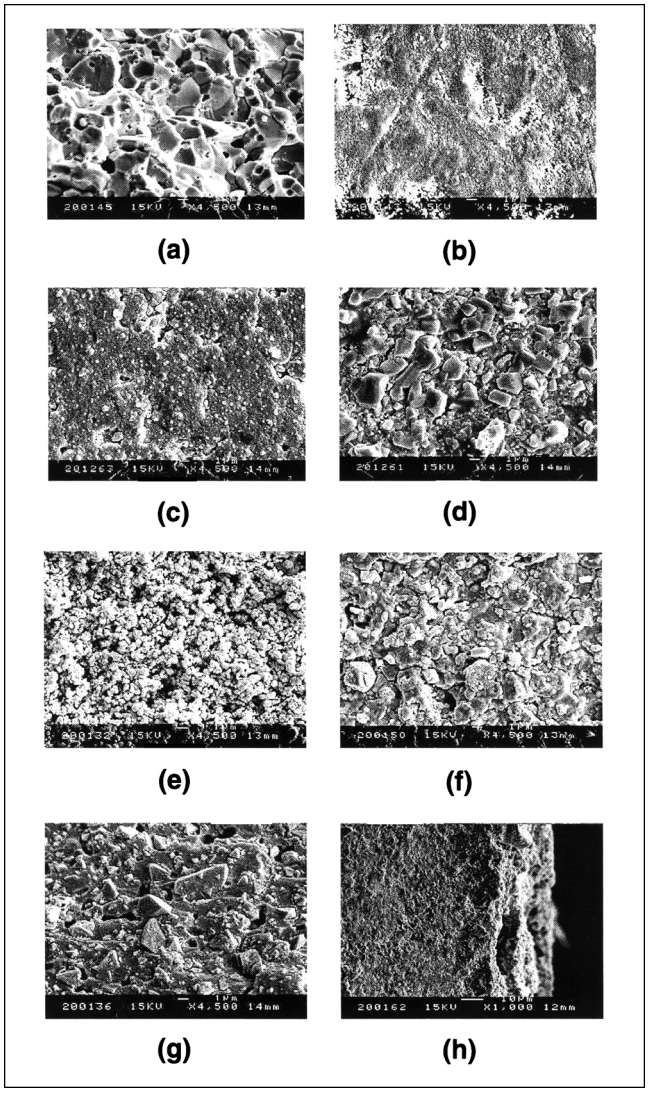

Figure 11. SEM of fresh and used membranes.

(a) The cross-section of fresh membrane; (b) the polished surface of fresh membrane; (c) the membrane surface exposed to reactive side in blank membrane reactor; (d) the membrane surface exposed to air side in blank membrane reactor; (e) the membrane surface exposed to reactive side in membrane reactor; (f) the membrane surface exposed to air side in membrane reactor; (g) the cross section of membrane center in membrane reactor; (h) the cross section near the reaction side in membrane reactor.

membrane packed with the catalyst, there was a porous layer found at the membrane surface exposed to the reaction side (Figure 11e). The porous layer could have caused the decomposition of the SCFZ in a strongly reducing atmosphere, and large grains at the membrane surface broke into many fine particles. The porous layer increased the surface area of the SCFZ membrane exposed to the reaction side, which would be beneficial to the oxygen permeation through the SCFZ membranes. Similar phenomena of this type of decomposition at a surface exposed to a reducing atmosphere were also observed by Tsai et al. (1997) and Xu and Thomson (1998) who, respectively, studied the $La_{0.2}Ba_{0.8}Fe_{0.8}Co_{0.2}O_{3-\delta}$ membrane for POM and $La_{0.6}Sr_{0.4}Co_{0.2}Fe_{0.8}O_{3-\delta}$ mem-

brane for OCM, reporting that these materials were subjected to severe degradation when exposed to a strongly reducing atmosphere. The thickness of the porous layer in Figure 11h was only about 10 μm, which was very similar to the result reported by Tsai (1997). It was found from Figure 11g that the structure of the bulk of the membrane used for the POM remained intact and dense. It can be seen in Figure 11d and 11f that after a lengthy operation, the etched membrane surface was developed at the air side by some big grains.

Conclusions

1. The perovskite-related SCFZ membrane reactors were used to study the POM. Three operational processes, including the oxygen permeation measurements, blank membrane reactor experiments, and membrane reactor experiments, were compared. The oxygen permeation measurements of the SCFZ membrane were performed in the air/helium gradient, and an apparent activation energy of 69 ± 5 kJ/mol was obtained in the temperature range of 1,023−1,223 K. In the air/helium gradient, the oxygen permeation of the SCFZ membrane was controlled by both the bulk diffusion and surface exchange rate.

2. The membrane reactor without catalyst packing was operated continuously for over 270 h. The main products were CO_2 and H_2O, which were produced at the membrane surface exposed to the reaction side. An increase in the oxygen flux in the membrane reactor without catalyst could be attributed to the increase in the catalytic activity at the membrane surface. The steady-state oxygen flux was about twice the value under the air/helium gradient. The membrane reactor packed with NiO/Al_2O_3 catalyst was continuously operated for over 220 h at constant operation conditions. The methane conversion was achieved at about 64% with 100% CO selectivity after steady state was reached. The oxygen flux increased gradually to about 4.5 $cm^3(STP)/min \cdot cm^2$, which was about ten times the value under the air/helium gradient.

3. The effect of the variation in the helium flow rate on the oxygen permeation flux was investigated for three operational processes, including the permeation measurements, blank membrane reactor, and membrane reactor. The increase in the helium flow rate resulted in an increase in the oxygen flux in the air/helium gradient. However, a decrease in the oxygen flux was found in the membrane reactors when the helium flow rate was increased. The oxygen flux in the membrane reactor packed with the catalyst was affected by the partial pressure of the feed gas CH_4, and an increase in the CH_4 partial pressure resulted in an increase in the oxygen flux in the membrane reactor. The results also showed that the oxygen flux of the SCFZ membrane in reducing atmosphere could be limited by the surface reaction rate at the reaction side of the membrane.

4. After a lengthy operation, a slight structural change in the membrane surface at the reaction side was found in the membrane reactor without catalyst packing. For the membrane reactor packed with NiO/Al_2O_3, a porous layer was developed at the surface of the SCFZ membrane exposed to the reaction side after a lengthy operation.

Acknowledgment

We acknowledge the support of the National Natural Science Foundation of China (NNSFC, No. 20125618) and Key Laboratory of Chemical Engineering and Technology of Jiangsu Province.

Notation

A = perexponential, mol/m·s·K
E_a = activation energy for diffusion of oxygen, kJ/mol
F = Faraday constant, 96,485 C/mol
F_i = molar flow rate of species i, mol/s
$F_{i,\text{inlet}}$ = molar flow rate of species i at the inlet of reactor, mol/s
$F_{i,\text{outlet}}$ = molar flow rate of species i at the outlet of reactor, mol/s
$\dot{h}$ = free-electron hole
J_{O_2} = oxygen permeation flux, $cm^3(STP)/min \cdot cm^2$
L = thickness of membrane, mm
O_O^X = oxygen ion on its normal lattice position
P_{CH_4} = methane partial pressure, Pa
P_{O_2} = oxygen partial pressure, Pa
P'_{O_2} = oxygen partial pressure at high-pressure side of membrane, Pa
P''_{O_2} = oxygen partial pressure at low-pressure side of membrane, Pa
Q_i = volume flow rate of species i at the inlet of reactor, $cm^3(STP)/min$
R = gas constant, 8.314 J/mol·K
S_{CO} = CO selectivity
t = reaction time, h
t_{el} = electronic transference number
T = temperature, K
$V_O^{\cdot\cdot}$ = oxygen ion vacancy
X_{CH_4} = CH_4 conversion

Greek letters

σ_{ion} = ion conductivity, S/m

Literature Cited

Alqahtany, H., D. Eng, and M. Stoukides, "Synthesis Gas Production from Methane Over an Iron Electrode in a Solid Electrolyte Cell," *J. Electrochem. Soc.*, **140**, 1677 (1993).

Balachandran, U., J. T. Dusek, P. S. Maiya, B. Ma, R. L. Mieville, M. S. Kleefisch, and C. A. Udovich, "Ceramic Membrane Reactor for Converting Methane to Syngas," *Catal. Today*, **36**, 265 (1997).

Chen, C. H., H. J. M. Bouwmeester, R. H. E. van Doorn, H. Kruidhof, and A. J. Burggraaf, "Oxygen Permeation of $La_{0.3}Sr_{0.7}CoO_{3-\delta}$," *Solid State Ionics*, **98**, 7 (1997).

Dyer, P. N., R. E. Richards, S. L. Russek, and D. M. Taylor, "Ion Transport Membrane Technology for Oxygen Separation and Syngas Production," *Solid State Ionics*, **134**, 21 (2000).

Gellings, P. J., and H. J. M. Bouwmeester, "Solid State Aspects of Oxidation Catalysis," *Catal. Today*, **58**, 1 (2000).

Hendriksen, P. V., P. H. Larsen, M. Mogensen, F. W. Poulsen, and K. Wiik, "Prospects and Problems of Dense Oxygen Permeable Membranes," *Catal. Today*, **56**, 283 (2000).

Jin, W., S. Li, P. Huang, N. Xu, J. Shi, and Y. S. Lin, "Tubular Lanthanum Cobaltite Perovskite Membrane Reactors for Partial Oxidation of Methane to Syngas," *J. Memb. Sci.*, **166**, 13 (2000).

Kröger, F. A., *The Chemistry of Imperfect Crystals*, North-Holland, Amsterdam (1964).

Kruidhof, H., H. J. M. Bouwmeester, R. H. E. van Doorn, and A. J. Burggraaf, "Influence of Order-Disorder Transitions on Oxygen Permeability Through Selected Nonstoichiometric Perovskite-Type Oxides," *Solid State Ionics*, **63**, 816 (1993).

Lee, T. H., Y. L. Yang, A. J. Jacobson, B. Abeles, and M. Zhou, "Oxygen Permeation in Dense $SrCo_{0.8}Fe_{0.2}O_{3-\delta}$ Membranes: Surface Exchange Kinetics versus Bulk Diffusion," *Solid State Ionics*, **100**, 77 (1997).

Li, S., W. Jin, N. Xu, J. Shi, Y. S. Lin, M. Z.-C. Hu, and E. A. Payzant, "Comparison of Oxygen Permeability and Stability of Perovskite Type $La_{0.2}A_{0.8}Co_{0.2}Fe_{0.8}O_{3-\delta}$ (A = Sr, Ba, Ca) Membranes," *Ind. Eng. Chem. Res.*, **38**, 2963 (1999a).

Li, S., W. Jin, P. Huang, N. Xu, J. Shi, M. Z.-C. Hu, E. A. Payzant, and Y. H. Ma, "Perovskite-Related ZrO_2-Doped $SrCo_{0.4}Fe_{0.6}O_{3-\delta}$ Membrane for Oxygen Permeation," *AIChE J.*, **45**, 276 (1999b).

Li, S., W. Jin, N. Xu, and J. Shi, "Mechanical Strength, and Oxygen and Electronic Transport Properties of $SrCo_{0.4}Fe_{0.6}O_{3-\delta}$-YSZ Membranes," *J. Membr. Sci.*, **186**, 195 (2001).

Omata, K., S. Hashimoto, H. Tominaga, and K. Fujimoto, "Oxidative Coupling of Methane Using a Membrane Reactor," *Appl. Catal.*, **52**, L1 (1989).

Pei, S., M. S. Kleefisch, T. P. Kobylinski, J. Faber, C. A. Udovich, V. Zhang-McCoy, B. Dabrowski, U. Balachandran, R. L. Mieville, and R. B. Poeppel, "Failure Mechanisms of Ceramic Membrane Reactors in Partial Oxidation of Methane to Synthesis Gas," *Catal. Lett.*, **30**, 201 (1995).

Qiu, L., T. H. Lee, L. M. Liu, Y. L. Yang, and A. J. Jacobson, "Oxygen Permeation Studies of $SrCo_{0.8}Fe_{0.2}O_{3-\delta}$," *Solid State Ionics*, **76**, 321 (1995).

Sammells, A. F., M. Schwartz, R. A. Mackay, T. F. Barton, and D. R. Peterson, "Catalytic Membrane Reactors for Spontaneous Synthesis Gas Production," *Catal. Today*, **56**, 325 (2000).

Sanchez, J., and T. T. Theodore, "Current Developments and Future Research in Catalytic Membrane Reactors," *Fundamentals of Inorganic Membrane Science and Technology*, A. J. Buggraaf and L. Cot, eds., Elsevier, Amsterdam, p. 529 (1996).

Ten Elshof, J. E., H. J. M. Bouwmeester, and H. Verweij, "Oxygen Transport Through $La_{1-x}Sr_xFeO_{3-\delta}$ Membrane. I. Permeation in Air/He Gradients," *Solid State Ionics*, **81**, 97 (1995).

Teraoka, Y., H. M. Zhang, S. Furukawa, and N. Yamazoe, "Oxygen Permeation Through Perovskite-Type Oxides," *Chem. Lett.*, 1743 (1985).

Tsai, C.-Y., A. G. Dixon, W. R. Moser, and Y. H. Ma, "Dense Perovskite Membrane Reactors for the Partial Oxidation of Methane to Syngas," *AIChE J.*, **43**, 2741 (1997).

Van Hassel, B. A., J. E. ten Elshof, and H. J. M. Bouwmeester, "Oxygen Permeation Flux Through $La_{1-y}Sr_yFeO_{3-\delta}$ Limited by Carbon Monoxide Oxidation Rate," *Appl. Catal. A: General*, **119**, 279 (1994).

Wagner, C. "Equations for Transport in Solid Oxides and Sulfides of Transition Metals," *Prog. Solid State Chem.*, **10**, 3 (1975).

Xu, S. J., and W. J. Thomson, "Perovskite-Type Oxide Membranes for the Oxidative Coupling of Methane," *AIChE J.*, **43**, 2731 (1997).

Xu, S. J., and W. J. Thomson, "Stability of $La_{0.6}Sr_{0.4}Co_{0.2}Fe_{0.8}O_{3-\delta}$ Perovskite Membranes in Reducing and Nonreducing Environments," *Ind. Eng. Chem. Res.*, **37**, 1290 (1998).

Zeng, Y., Y. S. Lin, and S. L. Swartz, "Perovskite-Type Ceramic Membranes: Synthesis, Oxygen Permeation and Membrane Reactor Performance for Oxidative Coupling of Methane," *J. Memb. Sci.*, **150**, 687 (1998).

Manuscript received Aug. 21, 2001, and revision received Feb. 6, 2002.